J. Am. Chem. Soc. 1983, 105, 4767-4774

in 78% total yield (0.17 g) by column chromatography (silica gel, cyclohexane). The cis/trans isomer ratio was 2.5, indicating that the intermediate aldehyde was epimerized by the base.

Variable-Temperature NMR Measurement. Samples (ca. 10 mg) were dissolved in 0.4 mL of acetone-d_6. Using Me_4Si as an internal standard, NMR spectra were taken between 10 and -90 °C on a Varian XL200 FT-NMR spectrometer. The CLATUX program[21] was employed to analyze the line shapes of the methyl group resonance, which was observed as a singlet by the irradiation at the methine proton.

Acknowledgment. We thank Dr. Takuji Sugimoto, School of Medicine, Osaka University, for graciously providing the program for the computation of total delocalization energies and Dr. Nobuo Tanaka, Kyoto Institute of Technology, for helpful discussion on HPLC and graciously providing excellent reversed-phase HPLC columns packed by himself.

Registry No. **1a**, 85781-42-6; **1b**, 85781-43-7; **1c**, 85781-44-8; **1d**, 85781-45-9; **2a**, 85848-69-7; **2b**, 85848-70-0; **2c**, 85848-71-1; **2d**, 85848-72-2; **3a**, 85781-46-0; **3b**, 85781-47-1; **3c**, 85781-48-2; **3d**, 85781-49-3; **4a**, 85848-73-3; **4b**, 85848-74-4; **4c**, 85848-75-5; **4d**, 85848-76-6; **5**, 85781-50-6; **6**, 85848-77-7; **7**, 85781-51-7; **8**, 85848-78-8; **9**, 85781-52-8; **10**, 85848-79-9; 11, 85781-53-9; **12**, 85848-80-2; 13, 85781-54-0; **14**, 85848-81-3; **15**, 85781-55-1; **16**, 85848-82-4; St-C_3-St, 58845-03-7; St-C_4-St, 41996-99-0; St-C_5-St, 79541-69-8; St-C_6-St, 32927-54-1; *p*-methoxystyrene, 637-69-4; *p*-methylstyrene, 622-97-9; styrene, 100-42-5; *p*-chlorostyrene, 1073-67-2; *m*-(trifluoromethyl)styrene, 402-24-4; *p*-nitrostyrene, 100-13-0; indene, 95-13-6; 2-phenylpropene, 98-83-9; α-phenylstryene, 530-48-3; 1,3-cyclohexadiene, 592-57-4; *trans*-1,3-pentadiene, 2004-70-8.

Supplementary Material Available: Table of ^1H NMR and mass spectroscopic data of cyclophane (4 pages). Ordering information is given on any current masthead page.

Rate-Controlling Two-Proton Transfer Coupled with Heavy-Atom Motion in the 2-Pyridinone-Catalyzed Mutarotation of Tetramethylglucose. Experimental and Calculated Deuterium Isotope Effects

Kjell-Åke Engdahl,[1a] Håkan Bivehed,[1a] Per Ahlberg,*[1a] and William H. Saunders, Jr.*[1b]

Contribution from the Department of Organic Chemistry, University of Uppsala, S-751 21 Uppsala, Sweden, and the Department of Chemistry, University of Rochester, Rochester, New York 14627. *Received November 9, 1982*

Abstract: Primary and secondary deuterium isotope effects have been measured by polarimetry, and primary isotope effects have been calculated for the classical bifunctional catalysis: 2-pyridinone-catalyzed mutarotation of 2,3,4,6-tetra-*O*-methyl-α-D-glucopyranose (α-TMG) in benzene. From the positively curved plot of the specific rate of epimerization vs. the mole fraction of ^2H in the "pool" of OH and NH hydrogens, the isotope effects $k_{HH}/k_{DD} = 3.66 \pm 0.09$, $k_{HH}/k_{DH} = 1.5$, and $k_{HH}/k_{HD} = 2.4$ have been calculated. A secondary isotope effect of 1.14 ± 0.02 has been measured by using α-TMG and (1-^2H)-2,3,4,6-tetra-*O*-methyl-α-D-glucopyranose [(1-^2H)-α-TMG], the synthesis of which is described in detail, together with those for (*N*-^2H)-2-pyridinone and (1-*O*-^2H)-2,3,4,6-tetra-*O*-methyl-α-D-glucopyranose [(1-*O*-^2H)-α-TMG]. The rate data obtained have also been analyzed by fractionation theory, yielding approximately equal fractionation factors (0.5). The interpretation of the results has been assisted by calculations of the primary deuterium isotope effects using the BEBOVIB IV program. Two models involving small and considerable coupling, respectively, of the transferring protons to heavy-atom motion have been considered. In the favored structure for the transition state of the rate-limiting step, two protons are in transit, and their motion is governed either by a potential with a barrier or by one without. Their motion is considerably coupled to the heavy-atom motion (i.e., the breakage of the ring C–O bond), and tunnel corrections to the isotope effects are found to be negligible. The results uphold the principle behind the rule of the geometric mean, i.e., $(k_{HH}/k_{HD})(k_{HH}/k_{DH}) = k_{HH}/k_{DD}$, despite the strong couplings in the transition state. The calculated k_{HH}/k_{DD} values are found to be relatively insensitive to the extent and symmetry of the proton transfers.

Introduction

Thirty years ago Swain and Brown reported their discovery of the unusual catalytic activity of 2-pyridinone in the epimerization of α-TMG to β-TMG in benzene.[2] The extraordinary efficiency of this catalyst in relation to its weak basic and acidic properties was the basis for the formulation of the bifunctional mechanism shown in Scheme I. In the 2-pyridinone–hemiacetal (TMG) complex the two protons were assumed to be transferred simultaneously in the rate-controlling transition state. Since its discovery this type of catalysis has attracted considerable interest.[3]

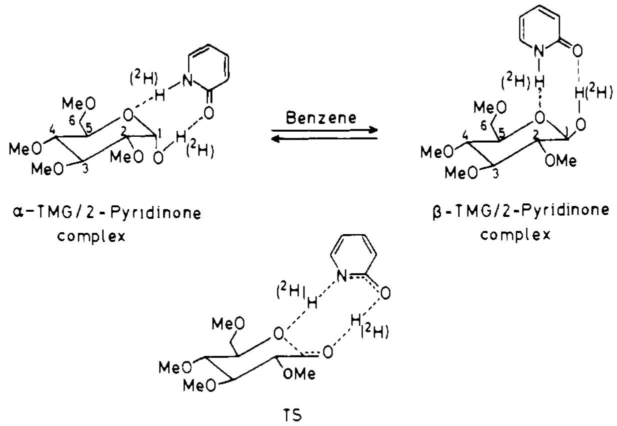

To obtain a deeper understanding of the nature of two-proton transfers in bifunctional catalysis, we are investigating a number of reaction systems. We have studied *sec*-amidine catalyzed 1,3-proton transfers in substituted propenes in which protons are transferred from carbon to nitrogen and from nitrogen to carbon

---

(1) (a) University of Uppsala. (b) University of Rochester.

(2) Swain, C. G.; Brown, J. F. *J. Am. Chem. Soc.* **1952**, *74*, 2538–2543.

(3) (a) Lowry, T. M.; Smith, G. F. *J. Chem. Soc.* **1927**, *129*, 2539–2554. (b) Swain, C. G.; Brown, J. F. *J. Am. Chem. Soc.* **1952**, *74*, 2534–2537. (c) Huang, H. H.; Robinson, R. R.; Long, F. A. *Ibid.* **1966**, *88*, 1866–1872. (d) Rony, P. R. *Ibid.* **1968**, *90*, 2824–2831. (e) Rony, P. R.; McCormack, W. E.; Wunderly, S. W. *Ibid.* **1969**, *91*, 4244–4251. (f) Rony, P. R. *Ibid.* **1969**, *91*, 6090–6096. (g) Rony, P. R.; Neff, R. O. *Ibid.* **1973**, *95*, 2896–2905. (h) Kergomard, A.; Lê Quang Xâng; Renard, M. F. *Tetrahedron* **1976**, *32*, 1983–1988. (i) Fiandanese, V.; Naso, E. *J. Chem. Soc., Perkin Trans. 2* **1977**, 1047–1051. (j) Kjaer, A. M.; Nielsen, H.; Sörensen, P. E.; Ulstrup, J. *Acta Chem. Scand., Ser. A* **1980**, *34*, 281–288. (k) Bell, R. P. "The Proton in Chemistry", 2nd ed.; Chapman and Hall: London, 1973; pp 183–190. (l) Jencks, W. P. "Cataysis in Chemistry and Enzymology"; McGraw-Hill: New York, 1969.

0002-7863/83/1505-4767$01.50/0

Scheme II

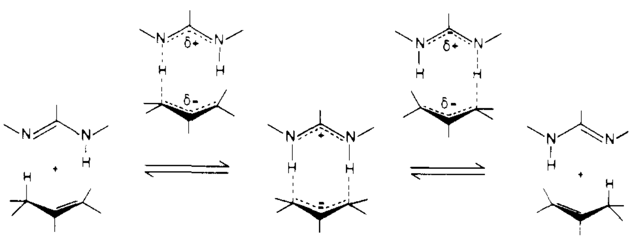

(Scheme II). Using ^{2}H labeling, isotope effects, and stereochemistry, it has been possible to show that the *sec*-amidine acts in a bifunctional manner and that the reaction occurs stepwise with rate-limiting single-proton transfer while the other proton might be hydrogen bonded in the transition state.[4] The behavior of this reaction system sharply contrasts that of the title reaction, in which protons are transferred between electronegative atoms only, i.e., between nitrogen and oxygen and between oxygen and oxygen.

The reaction system in question has recently been quantitatively reinvestigated with the use of microcalorimetry, and some new features have been revealed. Not only the thermodynamics but also the dynamics of the system have been measured with this technique.[5] TMG, previously assumed to be monomeric and complexed with 2-pyridinone, was found to be highly dimerized at concentrations commonly used in kinetic investigations. The equilibrium constant for its self-association and that of 2-pyridinone and the complexation constant for the 2-pyridinone–TMG complex were measured together with the thermodynamic parameters for the equilibria. The heats of reaction ($\Delta H°$) for these reactions show that the association complexes involve two hydrogen bonds and that they are therefore cyclic, as previously assumed. Also, the rate of epimerization, together with its small heat of reaction, was measured microcalorimetrically. These results prompted a revision of the previously reported[3d] free-energy diagram for the system.[5b]

However, several important aspects of the rate-controlling transition state of the title reaction remain to be clarified: Does the multiple proton transfer occur in an elementary reaction, i.e., are the protons transferred simultaneously, as suggested, or by a stepwise mechanism? To what extent are the proton transfers coupled to heavy-atom motion in the transition state? Is tunneling important in the reactions? Thus, various transition-state structures could be formulated, depending on the number of hydrogens and their degree of transfer and coupling to heavy-atom motion. A possible source of information about these questions are isotope effects.

In the present paper we provide a full report on measurements of primary and secondary deuterium isotope effects on the mutarotation in benzene.[6]

The primary deuterium isotope effects were extracted from the positively curved plot of the specific rate of epimerization vs. the mole fraction of ^{2}H in the pool of OH and NH hydrogens. The following values were obtained: $k_{HH}/k_{DD} = 3.66 \pm 0.09$, $k_{HH}/k_{DH} = 1.5$, and $k_{HH}/k_{HD} = 2.4$. The secondary deuterium isotope effect 1.14 ± 0.02 was measured by using (1-^{2}H)-2,3,4,6-tetra-*O*-methyl-α-D-glucopyranose [(1-^{2}H)-α-TMG]. The synthesis of this compound, together with those of (*N*-^{2}H)-2-pyridinone and (1-*O*-^{2}H)-2,3,4,6-tetra-*O*-methyl-α-D-glucopyranose [(1-*O*-^{2}H)-α-TMG], is also reported.

The interpretation of the primary isotope effects of this complex reaction has been assisted by calculations using the BEBOVIB IV program. The isotope effects are also analyzed by fractionation theory.

The results suggest that two hydrogens are in transit in the rate-controlling transition state and that each of them has a fractionation factor of about 0.5. These results, together with the calculations, favor a transition-state structure in which the simultaneous proton transfers are coupled with considerable heavy-atom motion (i.e., cleavage of the ring C–O bond). The tunnel correction to the isotope effects is found to be negligible. The calculations also show that, to a quite close approximation, the isotope effect for the dideuterated species is the product of the isotope effects for the two monodeuterated species in consistency with the experiments. Thus, the results uphold the principle behind the rule of the geometric mean despite strong coupling in the transition state. Another result of the calculations is that computed k_{HH}/k_{DD} values are relatively insensitive to the extent of proton transfer.

The two hydrogens in transit could in the transition state either be governed by a barrier, as assumed in our calculations, or, following Kreevoy and co-workers,[7] be transferred without any energy of activation.

Experimental Section

General Methods. The mutarotation rates were measured with a Perkin-Elmer 241 polarimeter equipped with an automatic data acquisition system, consisting of a Discan CM 4040 and a teletype unit. The water-jacketed polarimeter cell (optical path length 10 cm, volume 1 mL) was connected to a thermostat. The temperature was measured by means of a calibrated thermometer at the outlet of the cell with an accuracy of 0.02 °C.

The NMR spectra were obtained with JEOL JNM-FX100 or JNM-FX60 Fourier transform spectrometers equipped with 5- and 10-mm ^{1}H/^{13}C dual probes, respectively. Unless otherwise stated, the spectra were obtained by using the 100-MHz spectrometer. Mass spectra were obtained at 70 eV and 50 °C on an LKB 9000 mass spectrometer. Corrected melting points were measured with a melting point microscope.

The glassware—volumetric flasks, NMR tubes, etc.—were rinsed with absolute ethanol several times and dried at 150 °C for at least 15 h. While cooling to room temperature, they were thoroughly flushed with dry nitrogen and then transferred to the drybox. Syringes and the polarimetric cell were rinsed with absolute ethanol several times and then vacuum-dried (50 °C (7 Pa)[8]) for 4 h in a desiccator that, when cooled to ambient temperature, was filled with dry nitrogen.

Whenever possible, the preparations were performed in the drybox in an atmosphere of dry nitrogen. Contamination of reactants and solvents by moist air was otherwise prevented by means of dry nitrogen. The materials used in the kinetic measurements such as the prepared stock solutions, the dried solvents, and the samples of TMG and 2-pyridinone were stored under nitrogen in sealed flasks, which in turn had been placed in larger bottles filled with dry nitrogen and silica gel or 5-Å molecular sieves.

Materials. Tetramethylglucose[5b] (anomeric mixture) was sublimed twice at 90 °C (1.3 Pa). Silica gel 60, 70–230 mesh was from Merck, and sodium borodeuteride was from Ciba-Geigy (≥99 atom % ^{2}H). Boron trifluoride etherate (Baker) was purified as described by Zweifel and Brown.[9] Bis(2-methoxyethyl) ether (Kebo-Grave), predried over 4-Å molecular sieves, was stirred with calcium hydride for 24 h and distilled from the hydride. Tetrahydrofuran (Merck, analytical grade), predried over molecular sieves (4 Å), was passed through a column of activated aluminum oxide, stirred with calcium hydride for 24 h and distilled from the hydride in a nitrogen atmosphere. Diethyl ether used for column chromatography (Merck, >99%) was dried over molecular sieves (4 Å) and distilled in a nitrogen atmosphere. Hexane (Baker, >95%) was dried as described elsewhere.[5b] Benzene (Merck, analytical grade) was dried over molecular sieves (3 Å), shaken with 0.2% (v/v) ^{2}H$_2$O (Ciba-Geigy, >99.5 atom % ^{2}H), and distilled. A 70% middle fraction was dried twice (for 24 h each time) over molecular sieves (3 Å) and then distilled. (^{2}H$_6$)Benzene (Ciba-Geigy, >99 atom % ^{2}H) was dried over molecular sieves (4 Å) for 48 h, decanted, and distilled. The 90% middle fraction (bp 78.1 °C) was collected. Methan(^{2}H)ol (Ciba-Geigy, >99.5 atom % *O*-^{2}H). (^{2}H$_6$)Dimethyl sulfoxide, ((^{2}H$_6$)Me$_2$SO

---

[4] (a) Ahlberg, P.; Ladhar, F. *Chem. Scr.* **1973**, *3*, 31–36. (b) Niemeyer, H. M.; Ahlberg, P. *J. Chem. Soc., Chem. Commun.* **1974**, 799–800. (c) Niemeyer, H. M.; Goscinsky, O.; Ahlberg, P. *Tetrahedron* **1975**, *31*, 1699–1704. (d) Jannẽ, K.; Ahlberg, P. *J. Chem. Soc., Chem. Commun.* **1976**, 1040–1041. (e) Ek, M.; Ahlberg, P. *Chem. Scr.* **1980**, *16*, 62–63. (f) Ahlberg, P.; Ek, M. *J. Chem. Soc., Chem. Commun.* **1979**, 624–625.

[5] (a) Engdahl, K.-Å.; Ahlberg, P. *J. Chem. Res., Synop.* **1977**, 340–341. (b) Engdahl, K.-Å.; Bivehed, H.; Bohman, O.; Obenius, U.; Ahlberg, P. *Chem. Scr.* **1981**, *18*, 176–183.

[6] Engdahl, K.-Å.; Bivehed, H.; Ahlberg, P.; Saunders, W. H., Jr. *J. Chem. Soc., Chem. Commun.* **1982**, 423–425.

[7] Eliason, R.; Kreevoy, M. M. *J. Am. Chem. Soc.* **1978**, *100*, 7037.

[8] 1 mmHg = 133 Pa.

[9] Zweifel, G.; Brown, H. C. *Org. React.* **1963**, *13*, 1–54.

Scheme III

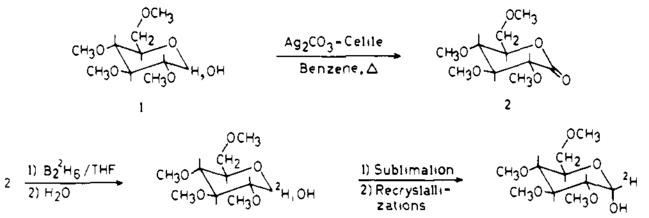

Ciba-Geigy, >99.5 atom % ^{2}H) was subjected to a three-stage static drying over molecular sieves (3 Å).[10] The water OH resonance in the ^{1}H NMR spectrum was then not detectable (S/N = 60 for the central peak of the $(^{2}H_{5})Me_{2}SO$ quintet), which means that the concentration of $^{1}HO^{2}H$ was less than 5×10^{-4} M. 2-Pyridinone (Fluka AG, purum grade) was sublimed twice (80 °C (7 Pa)) and then recrystallized from benzene. Water was removed azeotropically by distilling off 25% of the benzene from the solution before crystallization. The crystals were freed from remaining benzene in vacuum (7 Pa) at ambient temperature for 12 h. α-TMG was prepared as in ref 5b.

Syntheses. (N-^{2}H)-2-Pyridinone. Purified 2-pyridinone (1 g) was dissolved in 2 mL of methan(^{2}H)ol in a glass-stoppered sublimation apparatus containing dry nitrogen. The apparatus was placed in a plastic bag containing dry nitrogen at a pressure slightly above ambient. The methanol was evaporated from the stirred solution in oil pump vacuum. This hydrogen-exchange procedure was repeated twice. Traces of methanol were removed in vacuum (7 Pa) at room temperature over 6 h. Analysis by ^{1}H NMR in $(^{2}H_{6})Me_{2}SO$ showed that, of the exchangeable hydrogens, 97.6 atom % were ^{2}H.

(1-O-^{2}H)-2,3,4,6-Tetra-O-methyl-α-D-glucopyranose. Anomerically pure α-TMG[5b] (1 g) was dissolved at about −10 °C in 1.5 mL of cooled (−10 °C) methan(^{2}H)ol in a nitrogen-filled glass-stoppered sublimation apparatus placed in a plastic bag containing dry nitrogen at a pressure slightly above ambient. The methanol was evaporated (oil pump) from the stirred solution, the temperature being kept at about −10 °C. This hydrogen-exchange procedure was repeated twice. Traces of methanol were removed in vacuum (25 °C (7 Pa)) over 4 h. The product, (1-O-^{2}H)-α-TMG, was anomerically pure and contained 98.0 atom % ^{2}H bonded to 1-O (^{1}H NMR with $(^{2}H_{6})Me_{2}SO$ as solvent).

(1-^{2}H)-2,3,4,6-Tetra-O-methyl-D-glucopyranose. A synthesis according to Scheme III was developed for this compound.

2,3,4,6-Tetra-O-methyl-D-glucono-1,5-lactone (2).[11,12] Celite (60.0 g) was mixed with 120 mL of a solution of 9:1 methanol and concentrated hydrochloric acid (v/v). The mixture was stirred at room temperature for 10 min and then filtered on a sintered glass funnel. The Celite was washed with 2 × 20 mL of the methanol–hydrochloric acid solution and then with distilled water until the filtrate became neutral. Silver nitrate, 64.7 g (0.381 mol), was dissolved in 300 mL of distilled water in the dark and mixed with the washed Celite. Sodium carbonate ($10H_{2}O$; 57.2 g (0.200 mol)) dissolved in 500 mL of distilled water was transferred to the Celite–silver nitrate suspension. The mixture was stirred at room temperature for 15 min and then filtered on a sintered glass funnel. The now yellowish Celite was washed with distilled water until the filtrate became neutral and then was sucked dry. The remaining yellow-green mass was slowly dried in the dark at 60 °C on a rotatory evaporator.

Tetramethylglucose (1; 3.00 g (0.0127 mol)) was dissolved in 300 mL of benzene in a 500-mL round-bottomed flask equipped with a magnetic stirrer bar, a water separator, and a reflux condenser. The dried silver carbonate–Celite was added to the stirred solution, and the mixture was refluxed for 1 h. The black suspension was cooled and then filtered with a sintered glass funnel. The Celite was washed with 8 × 50 mL of dry benzene. The combined colorless filtrates were evaporated and the crude lactone (2) was isolated as a colorless oil, yield 2.83 g (95.1%). The lactone was taken up in 3.0 mL of dry diethyl ether and transferred to a chromatographic column charged with silica gel suspended in diethyl ether (46 × 4 cm). Elution with diethyl ether afforded the lactone as the first fraction. Evaporation of the ether gave 2.68 g (90.1%) of the pure lactone (**2**, $n^{24}{}_{D}$ 1.4530), which was stored over molecular sieves (4 Å); ^{1}H NMR [60 MHz, $(^{2}H_{6})Me_{2}SO$, 99.5 atom % ^{2}H, Ciba-Geigy, dried over molecular sieves (4 Å), internal reference $(^{2}H_{5},{}^{1}H)Me_{2}SO$, δ 2.50] δ 3.31 (s, OCH_{3}), 3.40 (s, OCH_{3}), 3.43 (s, OCH_{3}), 3.45 (s, OCH_{3}), 3.53–4.03 (complex), 4.43 (dt, C-5-H); ^{13}C NMR [60 MHz, $(^{2}H_{6})Me_{2}SO$, 99.5 atom % ^{2}H, Ciba-Geigy, dried over molecular sieves (4 Å), internal reference $(^{2}H_{6})Me_{2}SO$, δ 39.6] δ 168.7 (C-1), 81.2, 78.8, 77.3, 76.9, 70.8, 58.5 (OCH_{3}), 57.9 (OCH_{3}). The resonances of the four OCH_{3} groups are found in the region δ 57–59.

(1-^{2}H)-2,3,4,6-Tetra-O-methyl-D-glucopyranose (3). $(^{2}H_{6})$Diborane was generated externally from sodium borodeuteride and boron trifluoride etherate by the method used for synthesis of "light" diborane by Zweifel and Brown.[9] A solution of 2.0 g (0.0478 mol) of sodium borodeuteride in 50 mL of dry bis(2-methoxyethyl) ether was carefully added to a mixture of 16 mL of freshly distilled boron trifluoride etherate and 11 mL of dry bis(2-methoxyethyl) ether over 50 min. The $(^{2}H_{6})$diborane evolved was passed by a gentle stream of nitrogen via a Liebig condenser and through a sintered glass dispersion tube immersed into a stirred solution of 2.07 g (0.008 84 mol) of the lactone **2** in 50 mL of dry tetrahydrofuran. When the addition of the sodium borodeuteride solution was completed, the stirring was continued for another 50 min. Then the diborane generator was warmed up to and kept at 75–80 °C for 1.5 h. During the entire reduction the temperature of the lactone solution remained at 20–25 °C. The flask containing the reduced lactone was disconnected from the diborane generator, and the stirring was continued under nitrogen at room temperature. After 14 h, 7.0 mL of distilled water was carefully added. The mixture was stirred for 2 h and then transferred to a 200-mL round-bottomed flask. The solution was evaporated, and the residue was then taken up in three consecutive cycles in 30 mL of methanol and evaporated to dryness. The resulting crystal mass was dried in a vacuum desiccator over silica gel for 2 days. The dried crude product was sublimed (90 °C (1.3 Pa)) and a pure anomeric mixture of **3** (60.6 ± 0.1% α-anomer by ^{1}H NMR) was isolated; yield 2.00 g (95.4%, based on the purified lactone **2**); ^{1}H NMR [60 MHz $(^{2}H_{6})Me_{2}SO$, 99.5 atom % ^{2}H, Ciba-Geigy, dried over molecular sieves (4 Å), internal reference $(^{2}H_{5},{}^{1}H)Me_{2}SO$, δ 2.50] 2.78–3.21 (complex), 3.26 (s, C-6-α,β-OCH_{3}), 3.32 (s, C-2-α-OCH_{3}), 3.40 (s, C-4-α,β-OCH_{3}), 3.45 (s, C-3-α,β-OCH_{3}), 3.47 (s, C-2-β-OCH_{3}), 3.60–3.82 (complex), 6.40 (s, C-1-α-OH), 6.79 (s, C-1-β-OH).

(1-^{2}H)-2,3,4,6-Tetra-O-methyl-α-D-glucopyranose (4). The α-anomer **4** was isolated from **3** by repeated recrystallization from dry hexane. The crystal mass was dissolved in boiling hexane (100 mL/g) under a nitrogen atmosphere. Before crystallization, 25 % of the hexane was distilled off (to remove traces of methanol and water azeotropically). Crystallization commenced spontaneously after 30 min at room temperature, and after another 30 min the solution was cooled to 5 °C for 2 h. The hexane was sucked off under a nitrogen atmosphere, and the recrystallization was repeated. Pure **4** was isolated as a voluminous white crystal mass of thin needles after ten recrystallizations; yield 38.4% (based on the purified lactone **2**); mp 93–99 °C (see comment in ref 5b); $[\alpha]^{25}{}_{589}$ +124.5° (c 2, benzene), $[\alpha]^{25}{}_{578}$ +129.4° (c 2, benzene); isotopic purity, 98.9 ± 0.1% C-1-^{2}H (by ^{1}H NMR); ^{1}H NMR [$(^{2}H_{6})Me_{2}SO$, 99.5 atom % ^{2}H, Ciba-Geigy, dried over molecular sieves (4 Å), internal reference $(^{2}H_{5},{}^{1}H)Me_{2}SO$, δ 2.50] δ[13] 2.84–3.03 (complex), 3.25 (s, C-6-OCH_{3}), 3.32 (s, C-2-OCH_{3}), 3.40 (s, C-4-OCH_{3}), 3.45 (s, C-3-OCH_{3}), 3.67 (dt, C-5-H), 6.40 (s, C-1-α-OH); ^{13}C NMR [$(^{2}H_{6})Me_{2}SO$, 99.5 atom % ^{2}H, Ciba-Geigy, dried over molecular sieves (4 Å), internal reference $(^{2}H_{6})Me_{2}SO$, δ 39.6] δ 57.13, 58.33, 59.58, 59.73, 68.88, 71.41, 79.35, 81.29, 82.38 (all singlets), 88.61 (br t of low intensity, C-1); MS [70 eV, 50 °C], m/e (relative intensity) 188 (0.2), 163 (0.3), 162 (0.2), 160 (0.7), 159 (0.2), 158 (0.7), 145 (0.7), 143 (0.5), 136 (0.2), 132 (0.4), 131 (0.8), 130 (0.4), 129 (0.2), 128 (0.5), 127 (2), 119 (0.2), 118 (0.7), 117 (0.7), 116 (0.5), 115 (0.5), 114 (0.5), 113 (0.4), 112 (0.3), 111 (0.3), 103 (1), 102 (13), 101 (100), 100 (1), 99 (2), 90 (3), 89 (7), 88 (44), 87 (3), 85 (2), 76 (1), 75 (14), 74 (4), 73 (10), 72 (3), 71 (12), 69 (1), 60 (2), 59 (4), 58 (2), 57 (2), 56 (1), 55 (2), 53 (1), 47 (1), 46 (3), 45 (29), 44 (1), 43 (4), 42 (2), 41 (5), 39 (2), 34 (1), 33 (2), 32 (2). Only peaks larger than 1% (0.2% m/e 105–300) of the base peak are given.

Note: The observed mass spectrum (50 °C) for (1-^{2}H)-α-TMG is not in agreement with that reported by Kochetkov et al.[14,15] for an anomeric mixture of TMG at 175 °C. An investigation was therefore undertaken. Mass spectra of α-TMG,[5b] an anomeric mixture of TMG (62.0 ± 0.1% α-anomer by ^{1}H NMR) and methyl 2,3,4,6-tetra-O-methyl-α-D-glucopyranoside[5b] (α-PMG), respectively, were recorded under the same conditions as given for (1-^{2}H)-α-TMG. The two TMG samples gave essentially the same fragment pattern as (1-^{2}H)-α-TMG with the base peak at m/e 101. α-PMG, however, showed the base peak at m/e 88, and the fragment pattern was here in good agreement with the results given by Kochetkov et al. for the same compound. The discrepancy may

---

[10] Burfield, D. R.; Smithers, R. H. *J. Org. Chem.* **1978**, *43*, 3966–3968.

[11] Morgenlie, S. *Acta Chem. Scand., Ser. B* **1971**, *25*, 1154–1155.

[12] Balogh, V.; Fetizon, M.; Golfier, M. *Angew. Chem.* **1969**, *81*, 423–424.

[13] Casu, B.; Reggiani, M.; Gallo, G. G.; Vigevani, A. *Tetrahedron* **1968**, *24*, 803–821.

[14] Kochetkov, N. K.; Wulfson, N. S.; Chizhov, O. S.; Zolotarev, B. M. *Ibid.* **1963**, *19*, 2209–2224.

[15] Kochetkov, N. K. *J. Sci. Ind. Res.* **1964**, *23*, 468–471.

Table I. Kinetic Data for 2-Pyridinone-Catalyzed and Uncatalyzed Mutarotation of α-TMG and (1-^{2}H)-α-TMG at Different Isotopic Composition of the Pool of Nitrogen- and Oxygen-Bonded Hydrogens in Benzene and/or ($^2H_6$)Benzene at 24.98 ± 0.03 °C

entry	[TMG],[a] M	[2-pyridinone],[a] M	mole fraction ^{2}H of O- and N-bonded H	$10^6 k_{obsd}$, s^{-1}	accuracy (precision) of k_{obsd}, %
1[e]	0.0993	0.0500	0	1850[b]	0.65 (0.1)
2[e]	0.0993	0.0501	0.327 ± 0.002	1330[b]	0.65 (0.3)
3[e]	0.0995	0.0500	0.652 ± 0.004	886[b]	0.65 (0.3)
4[e]	0.0995	0.0501	0.979 ± 0.006	525[b]	0.65 (0.5)
5[e]	0.1000[c]	0.0500	0	1625[d]	0.65 (0.07)
6	0.1000	0.0500	0	1852[d]	0.65 (0.3)
7	0.15	0	0	3.8[d]	
8	0.10	0	0.980	0.85[d]	

[a] 1% relative error in concentration values. [b] Solvent ($^2H_6$)benzene. [c] 99.0 ± 0.1 atom % (1-^{2}H). [d] Solvent ($^1H_6$)benzene. [e] Duplicate runs.

be caused by the lower thermal stability of TMG in relation to PMG. Mass spectra are available from us upon request.

Kinetics. For the primary deuterium isotope effect measurements, stock solutions 0.1985 ± 0.0006 and 0.1991 ± 0.0006 M in (1-*O*-^{1}H)-α-TMG and (1-*O*-^{2}H)-α-TMG, respectively, and 0.1000 ± 0.0003 and 0.1002 ± 0.0003 M in (*N*-^{1}H)- and (*N*-^{2}H)-2-pyridinone, respectively, were prepared with ($^2H_6$)benzene as solvent. These stock solutions were stored in the freezer at about −25 °C. The deuterated solvent was used because it was originally planned to determine the degree of deuteration in the system after each polarimetric run by ^{1}H NMR using the deuterium resonance of ($^2H_6$)benzene for the purpose of internal lock. These attempts were not successful due to the extremely broadened signal of the exchangeable hydrogens in this solvent. In connection with a kinetic run, TMG and 2-pyridinone solutions were taken from the freezer and allowed to reach thermal equilibrium in the nitrogen-filled drybox. By means of a gas-tight syringe, a volumetric flask was charged with 0.800 ± 0.003 mL of the TMG solution and then stoppered. Another gas-tight syringe was filled with 2-pyridinone solution and a third with drybox atmosphere. The flask and the two latter syringes were immediately brought from the drybox to the polarimeter, where 0.800 ± 0.003 mL of the 2-pyridinone solution was delivered from the syringe to the flask containing the TMG solution. The start of the reaction was taken to be the time when half of the catalyst had been added. After agitation, the reaction mixture was transferred to the polarimeter cell by means of the nitrogen-filled syringe. The first rotations were typically measured 100–120 s after the start of the reaction. Data from the runs are collected in Table I.

In the secondary α-deuterium isotope effect measurements, equal amounts of (1-^{1}H)-α-TMG or (1-^{2}H)-α-TMG were weighed into volumetric flasks, which were filled to the mark with a benzene stock solution of 2-pyridinone from a gas-tight syringe. After agitation, the reaction mixture, 0.1 M in TMG and 0.05 M in 2-pyridinone, was transferred to the polarimetric cell (Table I).

Error Estimations. The error limits given are conservative, i.e., unless otherwise stated, they are maximum errors. The accuracies of the rate constants were obtained by propagating the concentration errors through the calculations.[5b] The standard error in the observed rate constants, obtained by linear least-squares regression analysis, was found to be small in comparison with the above error caused by the concentration errors.

Results

Results from the experiments are presented in this section, and results of the model calculations in the next.

Rate data, i.e., ln ($\alpha_t - \alpha_\infty$) vs. t plots for the 2-pyridinone-catalyzed mutarotation of TMG in ($^2H_6$)benzene at four different values of the atom fraction of ^{2}H (X_D) in the pool of mobile nitrogen- and oxygen-bonded hydrogens, are shown in Figure 1. The correlation coefficients of the linear least-squares fits to these semilogarithmic plots are 0.999 93 in two cases and 0.999 97 or larger in the remaining six. This, together with the absence of any sign of curvature in the plots, demonstrates the strictly pseudo-first-order nature of the reaction. Reaction conditions and calculated rate parameters (k_{obsd}) are shown in entries 1–4 in Table I. This set of measurements in Table I was carried out in the order presented, was duplicated once, and was completed within 7 days. The reason two lines within a pair do not coincide is mainly due to errors in the reaction starting time (t_0) of about 10 s. The very good reproducibility shows that the isotopic composition of the stock solutions remained unchanged during the period of measurements. The absence of any solvent isotope effect is indicated by the similarity of the k_{obsd} values of entries 1 and 6 in Table I. No corrections for blank mutarotation rates (entries 7 and 8) were made since these were found to be negligible, compared with corresponding rates obtained with 2-pyridinone as catalyst (entries 1 and 4).

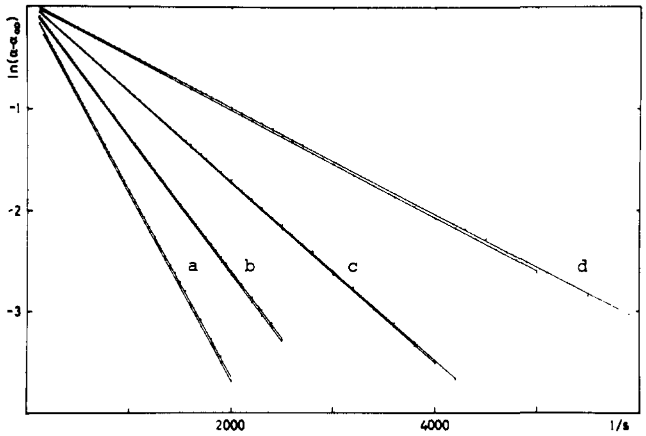

Figure 1. Plots of ln ($\alpha_t - \alpha_\infty$) vs. t for the mutarotation of TMG catalyzed by 2-pyridinone in ($^2H_6$)benzene at 24.98 ± 0.03 °C at four values of X_D, the atom fraction of ^{2}H in the mobile hydrogen pool: (a) 0; (b) 0.327; (c) 0.652; (d) 0.979.

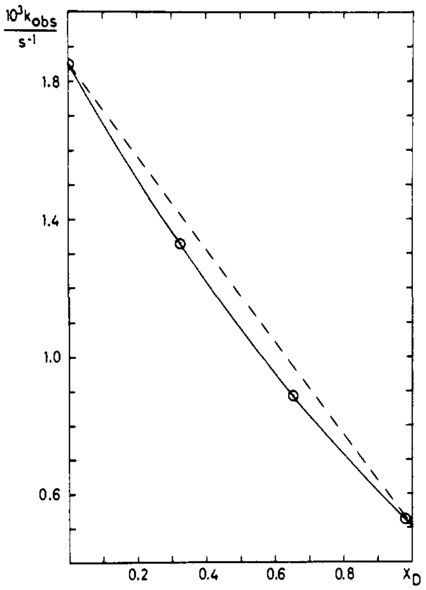

Figure 2. Plot of k_{obsd} vs. X_D, the mole fraction of X_D in the mobile hydrogen pool in benzene, at 24.98 ± 0.03 °C. The encircled points are experimental values. The solid and dashed lines have been simulated with the pairs of fractionation factors 0.65, 0.42 and 1.00, 0.27, respectively.

The nonlinear dependence of k_{obsd} on X_D is shown in Figure 2. This curved plot is conveniently analyzed by fractionation theory. In fractionation experiments one usually makes use of a large pool (bulk) of hydrogens, e.g., by using ^2H_2O as solvent. This choice implies some simplifications in the interpretations of the data obtained.[16] However, in the present case no such large pool is present, and therefore the relatively low concentration of oxygen-bonded hydrogens in monomeric TMG has arbitrarily been chosen as the bulk. A consequence of this is that the atom fraction of ^{2}H in this bulk (y) is not necessarily equal to X_D. These atom fractions are equal only if the fractionation factor for the exchange between the reactants (ϕ_r) defined by eq 1 is equal to 1. It should be mentioned that the rate of exchange of nitrogen- and oxygen-bonded hydrogens was found to be much faster than the mutarotation rate, as demonstrated by broad ^{1}H NMR resonances from these hydrogens. Py(H), Py(D), TMG(H), and TMG(D) denote 2-pyridinone and α-TMG with their respective exchangeable hydrogen being ^{1}H or ^{2}H. The two fractionation factors ϕ_{A1} and ϕ_{A2} for the activated complex, TMG,Py(H,H)‡, are defined by eq 2 and 3.

$$\mathrm{Py(H)} + \mathrm{TMG(D)} \overset{\phi_r}{\rightleftharpoons} \mathrm{Py(D)} + \mathrm{TMG(H)} \quad (1)$$

$$\mathrm{TMG,Py(H,H)}^{\ddagger} + \mathrm{TMG(D)} \overset{\phi_{A1}}{\rightleftharpoons} \mathrm{TMG,Py(D,H)}^{\ddagger} + \mathrm{TMG(H)} \quad (2)$$

$$\mathrm{TMG,Py(H,H)}^{\ddagger} + \mathrm{TMG(D)} \overset{\phi_{A2}}{\rightleftharpoons} \mathrm{TMG,Py(H,D)}^{\ddagger} + \mathrm{TMG(H)} \quad (3)$$

There are two fractionation factors for TMG,Py(H,H)‡ because it has two different exchangeable protons. The following formula (4) is easily derived by using the above definitions:

$$\frac{k_y}{k_0} = \frac{(1 - y + y\phi_{A1})(1 - y + y\phi_{A2})}{1 - y + y\phi_r} \quad (4)$$

The specific mutarotation rates at $y = 0$ and y are k_0 and k_y, respectively. The derivation of eq 4 is based upon the assumption that the fractionation factors for exchange of the second proton in TMG,Py(D,H)‡ and TMG,Py(H,D)‡ are ϕ_{A2} and ϕ_{A1}, respectively, i.e., the rule of the geometric mean[17] is assumed to be valid (cf. results of the model calculations). If $X_D = 1$, then y is also equal to 1 and eq 4 is simplified to $k_1/k_0 = \phi_{A1}\phi_{A2}/\phi_r$, and we calculate $k_1/k_0 = k_{obsd}(X_D = 1)/k_{obsd}(X_D = 0) = 0.273 \pm 0.007$ by using Table I and an extrapolated value of k_{obsd} to $X_D = 1$. The fractionation factor ϕ_r has been measured to be 1.0 ± 0.1 in Me$_2$SO by ^{1}H NMR, where the rate is low (on the NMR time scale) for the exchange of the 2-pyridinone and TMG hydrogens and two separate signals are therefore obtained for these hydrogens. Also, IR frequencies (KBr) indicate $\phi_r = 1$. We therefore assume that ϕ_r is equal to 1 under the experimental conditions of Table I, which implies that $X_D = y$, and calculate the following fractionation factors:

$$\phi_{A1} = 0.67,\ \phi_{A2} = 0.42 \text{ for } y = X_D = 0.327$$

$$\phi_{A1} = 0.64,\ \phi_{A2} = 0.43 \text{ for } y = X_D = 0.652$$

The average values $\phi_{A1} = 0.65$ and $\phi_{A2} = 0.42$ ($\phi_r = 1$) have been used in the simulation of the curved solid line in Figure 2.

According to the treatment of Albery, the curvature also indicates the number of fractionating sites in the transition state.[18] He defines a curvature parameter γ according to eq 5. In (5)

$$\gamma = 8 \ln (Y_{1/2}/Y_1^{1/2})/(\ln Y_1)^2 \quad (5)$$

$Y_{1/2}$ and Y_1 are the rate constant ratio k_y/k_0 at $y = {}^1/_2$ and 1, respectively (assuming $\phi_r = 1$ in our case). If an interpolated value of k_y at $y = {}^1/_2$, obtained from the k_{obsd} values of Table I, is used, $\gamma = 0.54$ may be calculated. Following Albery, the number of sites in the transition state must be greater than γ^{-1}, i.e., >1.85. This points at two fractionating hydrogens in the transition state.

Since the results of the model calculations of isotope effects in the next section have been expressed by using the specific rates k_{HH}, k_{HD}, k_{DH}, and k_{DD}, the connection with the fractionation factors above will be made. Equation 6 is valid when $\phi_r = 1$ and

$$k_{obsd} = k_{HH}X_H^2 + (k_{HD} + k_{DH})X_HX_D + k_{DD}X_D^2 \quad (6)$$

defines the specific rates. When $X_H = 1$ ($X_H = 1 - X_D$) $k_{obsd}(X_D = 0) = k_{HH}$, and at $X_H = 0$ $k_{obsd}(X_D = 1) = k_{DD}$. The following relations between isotope effects (inverted) and fractionation factors hold:

$$\phi_{A1} = k_{DH}/k_{HH} \qquad \phi_{A2} = k_{HD}/k_{HH} \qquad \phi_{A1}\phi_{A2} = k_{DD}/k_{HH}$$

With the above average fractionation factors, the following deuterium isotope effects are obtained:

$$k_{HH}/k_{DD} = 3.66 \pm 0.09 \qquad k_{HH}/k_{DH} = 1.5$$

$$k_{HH}/k_{HD} = 2.4$$

The errors in the latter two isotope effects or the fractionation factors ϕ_{A1} and ϕ_{A2} could be significant. Possible error sources are relative errors in the rate constants of Table I, deviation of ϕ_r from 1 in benzene, isotope effects on association equilibria, experimental errors in the isotopic composition of the reaction mixture, and an isotope effect on the lactam–lactim tautomerism of 2-pyridinone.

Calculations of maximal errors using the accuracy of the k_{obsd} of Table I show that errors as large as 20% could be present in the above fractionation factors. Using a ϕ_r of 0.8 instead of 1 changes the larger fractionation factor to 0.52 while the other remains at 0.42, i.e., a lower ϕ_r value makes the difference between the two ϕ_A values smaller. Only minor changes in the averages of the two fractionation factors result if isotope effects of 1.1 on the association equilibria are assumed. The assumed experimental errors in the isotopic composition also cause only minor changes. The isotope effect on the lactam–lactim tautomerism of 2-pyridinone was studied by ^{13}C NMR. Solutions of 2-pyridinone, (N-^{2}H)-2-pyridinone, and a mixture of 2-pyridinone and TMG in benzene gave essentially the same 2-pyridinone ^{13}C chemical shifts. This indicates either that mainly one of the tautomers is present in solution or, if the tautomeric equilibrium constant is not far from 1, that the isotope effect has to be close to 1. Comparison with ^{13}C NMR chemical shifts of 1-methyl-2-pyridinone and 2-methoxypyridine indicates that the equilibrium isotope effect is <1.1. According to Beak,[19] the favored tautomer in nonpolar solvents is 2-pyridinone and not 2-hydroxypyridine, which is dominating in the gas phase. The self-association (and possibly other associations) promotes the lactam form. Therefore, it seems likely that in our reaction system the main tautomer present is the lactam form 2-pyridinone.

A secondary deuterium isotope effect (1.14 ± 1.3%) on the epimerization of α-TMG was obtained by using (1-^{2}H)-α-TMG (entries 5 and 6 in Table I).

Model Calculations of Isotope Effects

In order to determine whether a simultaneous two-proton transfer could be consistent with relatively small primary deuterium isotope effects such as those reported here, we undertook model calculations. The cutoff model[20,21] shown in **5** retains all

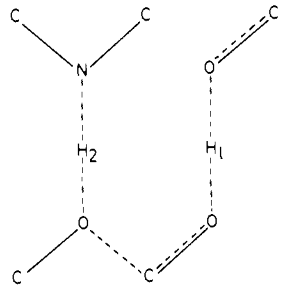

5

---

(16) Melander, L.; Saunders, W. H., Jr. "Reaction Rates of Isotopic Molecules"; Wiley: New York, 1980.

(17) Reference 16, p 209.

(18) Albery, W. J. In "Proton Transfer Reactions"; Caldin, E., Gold, V., Eds.; Chapman and Hall: London, 1975.

(19) Beak, P.; Covington, J. B.; Smith, S. G. *J. Am. Chem. Soc.* **1976**, *98*, 8284–8286.

Table II. Assumed Bond Lengths[a]

bond	r, Å	bond	r, Å
C–O	1.43	C–O	1.43
C–N	1.47	N–H	1.01
O–H	0.96		

[a] All are quoted as *single bond* lengths. In the models, the length is adjusted to the proper value for the given bond order by use of Pauling's rule (see text).

Table III. Assumed Force Constants

type	value,[a] mdyn/Å
O–H str	$7.8\, n_{OH}$
C–O str	$5.8\, n_{CO}$
N–H str	$7.8\, n_{NH}$
C–N str	$6.0\, n_{CH}$
O–H–O lin bd	$0.32\, n_{OH(1)} n_{OH(2)}$
O–H–N lin bd	$0.32\, n_{OH} n_{NH}$
C–O–H bd	$0.64\, n_{CO} n_{OH}$
O–C–O bd	$0.35\, n_{CO(1)} n_{CO(2)}$
C–O–C bd	$0.40\, n_{CO(1)} n_{CO(2)}$
C–N–H bd	$0.64\, n_{CN} n_{NH}$
C–N–C bd	$0.40\, n_{CN} n_{CN}$
C–N–H–O–C tors	0.02
H–O–C–O tors	0.10
O–C–O–H tors	0.02
C–O–H–O–C tors	0.02

[a] Bending and torsional force constants are multipled by $r_1 r_2$ (equilibrium bond lengths of the appropriate bonds) before the calculations. The bond orders (n) are those appropriate for the particular model. Hydrogen bonds in the reactant complex (carbonyl O of the 2-pyridinone to H of the substrate, and H of the 2-pyridinone to ether O of the substrate) are arbitrarily assigned bond orders of 0.05.

atoms within two bonds of the isotopically substituted protons. It differs from the transition state depicted in Scheme I in that the carbonyl and the amide NH groups of the 2-pyridinone are "disconnected" from one another. This is done so as to avoid the problems that arise in assigning off-diagonal elements in the force-constant matrix and obtaining a reasonable reaction coordinate for cyclic transition-state models.[22] This alteration in the model undoubtedly has some effect on the final numerical values but should not affect the qualitative conclusions. The reactant complex model is similar to the transition-state model shown in **5**, but with bond orders appropriate to the reactants. The bond orders in the reactant complex are arbitrarily set at 0.05 for the hydrogen bonds between the carbonyl oxygen of the 2-pyridinone and the hydroxyl proton of the substrate and between the N–H proton of the 2-pyridinone and the ether oxygen of the substrate.

The bond lengths used in the models either are taken from or are close to values in standard compilations (Table II).[23] Bond angles are arbitrarily set at 120° except for the 180° $N \cdots H_2 \cdots O$ and $O \cdots H_1 \cdots O$ angles. Although bond angles in the real system undoubtedly vary with extent of proton transfer in the transition state, the effect of this simplification on k_H/k_D should be small. Assumed force constants for the various stretching, bending, and torsional internal coordinates are listed in Table III. They are mostly obtained directly from, and in a few cases estimated from values in, literature compilations.[24-26]

The only off-diagonal elements in the force-constant matrix were those necessary to obtain an imaginary frequency for the vibrational mode representing the motion along the reaction coordinate. Reading along the reacting bonds from the upper left in **5**, these were $F_{NH,HO}$, $F_{HO,OC}$, $F_{OC,CO}$, $F_{CO,OH}$, and $F_{OH,HO}$. The values assigned them were calculated in the manner we have previously employed,[27-29] from eq 7–10.

$$F_{NH,HO} = A(F_{NH}F_{HO})^{1/2} \quad (7)$$

$$F_{HO,OC} = B(F_{HO}F_{OC})^{1/2} \quad (8)$$

$$F_{OC,CO} = C(F_{OC}F_{CO})^{1/2} \quad (9)$$

$$F_{CO,OH} = D(F_{CO}F_{OH})^{1/2} \quad (10)$$

$$F_{OH,HO} = E(F_{OH}F_{HO})^{1/2} \quad (11)$$

To reduce the number of parameters, the quantities A–E were divided into two sets: those involving primarily proton motion, for which $A = E$ was assumed, and those involving heavy-atom motion, for which $B = C = D$ was assumed. The relation between them then is given by

$$1 - 2A^2 - 3B^2 + 4A^2B^2 + B^4 + A^4 - A^4B^2 = F \quad (12)$$

where F is a curvature parameter, which must be negative in order to obtain an imaginary reaction coordinate frequency. The BEBOVIB IV program[30] was used to perform the calculations. It adjusts bond lengths to the appropriate values given the single-bond values (r_i^0) and the bond orders (n) as input, by using the Pauling relation:[31,32]

$$r_i = r_i^0 - 0.3 \ln n_i \quad (13)$$

Bond orders are also used to vary the force constants according to the relations in Table III. Conservation of total bond order to any given atom in the system of reacting bonds is assumed. Thus $n_{NH} + n_{HO} = 1$, $n_{HO} + n_{OC} = 1$, $n_{OC} + n_{CO} = 2$, and so on.

Before proceeding to the results of the calculations, a brief comment on the behavior of eq 12 would be appropriate. When A is large relative to B, the reaction coordinate motion involves mainly proton transfer. As B increases and A decreases, heavy-atom motion contributes increasingly to the reaction coordinate. For fairly large A (0.9–1.0) and small B (0.1–0.4), all solutions of eq 12 correspond to values of the curvature parameter, F, no more negative than −0.01. This signifies very slight curvature of the potential surface in the vicinity of the transition state and a consequently small tunnel correction.[33] If $B > A$, considerably more negative values of F are attainable (−0.35 for $A = 0.5$, $B = 0.8$, and −0.75 for $A = 0.3$ and $B = 0.95$), but the contribution of heavy-atom motion to the reaction coordinate is then so great that the sensitivity of the reaction coordinate frequency to isotopic substitution is slight. Even though tunneling can make a significant contribution to the *rate* in such cases, it contributes almost equally to the rates for the different isotopic species. The tunnel correction to the isotope effect thus remains negligible. We cannot exclude the possibility that the lack of significant tunnel corrections to the isotope effects calculated from our model arises from some artifact of the mathematical methods, but the small observed isotope effects certainly give no reason to suspect tunneling.

We carried out calculations for numerous sets of the parameters A, B, and F. Wide variation in the k_H/k_D values resulted, but for the purposes of the present discussion the range of results can

---

(20) Wolfsberg, M.; Stern, M. *J. Pure Appl. Chem.* **1964**, *8*, 225–242.

(21) Stern, M. J.; Wolfsberg, M. *J. Chem. Phys.* **1966**, *45*, 4105–4124.

(22) Keller, J. H.; Yankwich, P. E. *J. Am. Chem. Soc.* **1974**, *96*, 2303–2314.

(23) "Tables of Interatomic Distances and Configurations in Molecules and Ions"; Special Publications 11 and 18; The Chemical Society: London, 1958 and 1965.

(24) Wilson, E. B., Jr.; Decius, J. C.; Cross, P. "Molecular Vibrations"; McGraw-Hill: New York, 1965.

(25) (a) Schachtschneider, J. H.; Snyder, R. G. *Spectrochim. Acta* **1963**, *19*, 117–168. (b) Snyder, R. G.; Schachtschneider, J. H. *Ibid.* **1965**, *21*, 169–195.

(26) Herzberg, G. "Infrared and Raman Spectra"; Van Nostrand: Princeton, NJ, 1945.

(27) Katz, A. M.; Saunders, W. H., Jr. *J. Am. Chem. Soc.* **1969**, *91*, 4469–4472.

(28) Saunders, W. H., Jr. *Chem. Scr.* **1975**, *8*, 27–36.

(29) Reference 16, pp 64–66.

(30) Sims, L. B.; Burton, G.; Lewis, D. E. BEBOVIB IV, Program No. 337, Quantum Chemistry Program Exchange, Department of Chemistry, Indiana University, Bloomington, IN.

(31) Pauling, L. *J. Am. Chem. Soc.* **1947**, *69*, 542–553.

(32) Burton, G. W.; Sims, L. B.; Wilson, J. C.; Fry, A. *Ibid.* **1977**, *99*, 3371–3379.

(33) Reference 16, pp 13–17, 36–39.

Table IV. Model Calculations of Isotope Effects for the 2-Pyridinone-Catalyzed Mutarotation of Tetramethylglucose at 30 °C[a]

fraction of H transfer[b]	k_{HH}/k_{DH}[c]	k_{HH}/k_{HD}[d]	$(k_{HH}/k_{DH}) \times (k_{HH}/k_{HD})$	k_{HH}/k_{DD}[e]
(i) For $A = 0.95, B = 0.3, F = -0.0008$[f]				
0.1	2.59	2.78	7.20	7.20
0.3	5.12	6.24	31.95	31.92
0.5	7.17	9.13	65.46	65.41
0.7	5.34	7.41	39.57	39.50
0.9	2.81	4.28	12.03	12.03
(ii) For $A = 0.40, B = 0.65, F = -0.12$[f]				
0.1	1.50	1.58	2.37	2.38
0.3	1.62	1.96	3.18	3.18
0.5	1.65	2.21	3.65	3.64
0.7	1.65	2.39	3.94	3.95
0.9	1.59	2.42	3.85	3.85

[a] Calculated by using the model shown in 5 and the BEBOVIB-IV program.[30] See text for details. [b] Denotes the order of the forming bonds. It is assumed that H_1 and H_2 are equally transferred in all models. [c] H_1 in 5 is substituted by ^2H. [d] H_2 in 5 is substituted by ^2H. [e] H_1 and H_2 in 5 are substituted by ^2H. [f] A, B, and F are the parameters that determine the values of the off-diagonal elements in the force constant matrix according to eq 7-12.

be illustrated by two of the models: (i) $A = 0.95$, $B = 0.3$, $F = -0.0008$; (ii) $A = 0.40$, $B = 0.65$, $F = -0.12$. Calculated isotope effects for these two models are given in Table IV. Model i represents those cases where the reaction coordinate motion consists mainly of proton transfer, while model ii represents those cases where there is substantial heavy-atom motion in the reaction coordinate.

The most important conclusion to be drawn from Table IV is that, to a quite close approximation, the isotope effect for the dideuterated species is the product of the isotope effects for the two different monodeuterated species. Thus, the results uphold the principle behind the rule of the geometric mean,[34] which states that the isotope effect for a doubly labeled species is given by the product of the isotope effects for the corresponding singly labeled species. The principle is thus demonstrated to be applicable even when the motions of the two isotopically substituted atoms are rather strongly coupled in the transition state.

According to this result it should be entirely possible to observe unusually large primary deuterium isotope effects in a simultaneous two-proton transfer where both protons in transit are replaced by deuterons. It is equally true, however, that a large k_{HH}/k_{DD} value is not a necessary consequence of simultaneous transfer of two protons. When heavy-atom motion contributes substantially to the motion along the reaction coordinate, as in model ii, quite modest k_{HH}/k_{DD} values that are relatively insensitive to the extent of proton transfer can be observed. While model ii was chosen for illustration because it gives a maximum value of k_{HH}/k_{DD} close to the experimental isotope effect reported above, even smaller k_{HH}/k_{DD} values can be generated by further decreasing A, and larger values result when A is increased.

These findings further emphasize a point made previously by one of us,[35] that heavy-atom motion in the reaction coordinate is a fundamental source of variation in k_H/k_D. Although the flexibility of the model defeats any attempt at quantitative matching of observed and calculated isotope effects, it is at least clear that a transition state with substantial heavy-atom motion in the reaction coordinate is necessary for the observed isotope effect to be consistent with a simultaneous transfer of both protons. Another definite prediction of the model is that tunneling should make a negligible contribution to k_H/k_D in simultaneous two-proton transfers. The present experimental results are not inconsistent with this prediction, but further evidence would be desirable.

Scheme IV

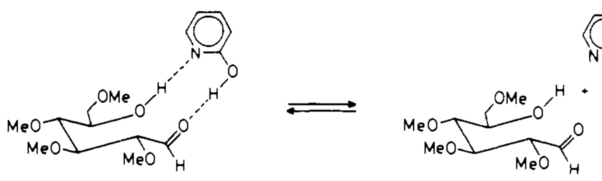

The calculations quoted so far have been made on the assumption that the fraction of proton transfer is the same for H_1 and H_2 in all models. It is entirely possible, however, for the two-proton transfers to be coupled in a single elementary step but to have occurred to different extents in the transition state. Consequently, we briefly explored a model in which H_2 transfer was in advance of H_1 transfer (0.5 for H_2, 0.1 for H_1 and so on up to 0.9 for H_2, 0.5 for H_1) but that was otherwise identical with model ii. The only difference in results was that the dependence of k_H/k_D on fraction of hydrogen transfer was even less marked than in model ii, k_{HH}/k_{DD} varying from 3.26 to 3.99. Thus there is no qualitative and little quantitative difference between synchronous and nonsynchronous coupled proton transfers.

Since the tautomer of 2-pyridinone, 2-hydroxypyridine, could be an active catalyst, some calculations were done on a model in which the C-N-C and C=O moieties (top part of **5**) were interchanged. The numerical results differed slightly from those in Table IV, but none of the qualitative conclusions is affected.

Discussion

In the following, our results will be analyzed in the light of the rate-limiting transition-state models: (a) the two protons are transferred simultaneously with or without being coupled to heavy-atom motion; (b) the two protons are governed by a potential having a barrier or are transferred without barrier control; (c) only one of the two protons is transferred with or without being coupled to heavy-atom motion.

The number of reaction steps in the epimerization process is most likely larger than indicated in Scheme I. Sugar chemistry suggests the presence of a hydroxy aldehyde intermediate formed by complete breaking of the ring C–O bond of the TMG,Py complex (Scheme IV). Thus, there are two transition states, one on each side of the open intermediate, and one of these leads to the α-TMG,Py complex and the other to the β-TMG,Py complex. Depending on the energy difference between them, either one or both are to be considered rate limiting. In any case, the transition states probably show many structural similarities.

Following a suggestion by a reviewer, the following derivation involving the aldehyde form as an intermediate is given:

$$\text{initial state} \underset{k_2}{\overset{k_1}{\rightleftharpoons}} \text{intermediate} \underset{k_4}{\overset{k_3}{\rightleftharpoons}} \text{final state}$$

The equilibrium constant for the epimerization K_{ep} is then given by $K_{ep} = k_1k_3/k_2k_4$. The observed rate constant is given by

$$k_{obsd} = k_1k_3/(k_2 + k_3) + k_4k_2/(k_2 + k_3) = k_1k_3(1 + 1/K_{ep})/(k_2 + k_3)$$

The deuterium isotope effect on the mutarotation will then be

$$\frac{k_{obsd}(H)}{k_{obsd}(D)} = \frac{k_{1H}}{k_{1D}} \frac{k_{3H}}{k_{3D}} \frac{k_{2D}}{k_{2H}} \frac{1 + k_{3D}/k_{2D}}{1 + k_{3H}/k_{2H}} \frac{1 + 1/K_{ep}(H)}{1 + 1/K_{ep}(D)}$$

This expression reduces to $k_{obsd}(H)/k_{obsd}(D) = k_{1H}/k_{1D}$ if (i) there is a negligible deuterium isotope effect on K_{ep} and (ii) the isotope effects on k_2 and k_3 are approximately the same. Both conditions are reasonable and are assumed in our treatment.

Heavy-atom motion in the rate-controlling transition state is indicated by the measured secondary α-deuterium isotope effect, 1.14 ± 0.02, which is caused by partial rehybridization at C-1 in the epimerization of (1-^{2}H)-α-TMG. Its magnitude suggests an intermediate cleavage of the ring C–O bond.[36]

---

(34) Bigeleisen, J. *J. Chem. Phys.* **1955**, *23*, 2264–2267.
(35) Reference 16, pp 152–154.
(36) Reference 16, p 172.

The interpretation of the primary isotope effects is more complex even though it has been simplified by using benzene as solvent. In this nonpolar solvent there is more control over the number of hydrogens involved in the rate-limiting transition state than, for example, in hydroxylic solvents in which hydrogens also participate in solvation. The measured isotope effects $k_{HH}/k_{DD} = 3.66 \pm 0.09$, $k_{HH}/k_{DH} = 1.5$, and $k_{HH}/k_{HD} = 2.4$ are all quite small, being primary deuterium isotope effects. A similar k_{HH}/k_{DD} value (3.5) for the same reaction has been reported in a review by Schowen.[37]

Results with two models studied in the calculations are presented in Table IV. These models assume simultaneous transfer of the two protons. The protonic motions are in model i essentially uncoupled and in model ii considerably coupled to heavy-atom motion in the TMG part of the transition state. The deuterium isotope effects obtained with i are much larger than those observed; for example, at a 0.5 fraction of H transfer $k_{HH}/k_{DD} = 65$, $k_{HH}/k_{DH} = 7$, and $k_{HH}/k_{HD} = 9$ are calculated. The choice of model ii on the other hand is strongly supported by the large secondary isotope effect observed. This model is able to reproduce the observed isotope effects closely; for example, at a 0.5 fraction of H transfer, $k_{HH}/k_{DD} = 3.6$, $k_{HH}/k_{DH} = 1.7$, and $k_{HH}/k_{HD} = 2.2$ are obtained. In the calculations the 2-pyridinone tautomer has been assumed to be the catalyst and the k_{HH}/k_{DH} and k_{HH}/k_{HD} values refer to transfers of deuteriums between O and O and N and O, respectively. It is therefore possible that the observed isotope effect 2.4 refers to the deuterium being transferred between N and O (Table IV). An important result of the calculations with ii is the rather small change in the isotope effects with fraction of H transfer. The fact that the calculated k_{HH}/k_{DH} and k_{HH}/k_{HD} differ from each other depends on the different values of n_{CO} (see **5** and Table III) and consequently different bending force constants for the $H_2\cdots O\cdots C$ and $H_1\cdots O\overset{\cdots}{-}C$ angles. The calculations also show that asymmetry in the simultaneous transfer of the hydrogens yields results close to those obtained experimentally. Another important result of the calculations is that, to a quite good approximation, the isotope effect for the dideuterated species is equal to the product of the isotope effects for the two different monodeuterated species. Thus, the calculation results uphold the principle behind the rule of the geometric mean.[34] The validity of this rule was assumed in the evaluation of the experimental isotope effects by the fractionation theoretical approach above.

It is also interesting to note that the calculations show that the tunnel correction to the isotope effects is negligible.

In the above discussion, the transfer of the two hydrogens has been assumed to be controlled by a barrier. However, following a most interesting suggestion by Kreevoy for the mechanism of acid-catalyzed acetal hydrolysis, another mechanistic possibility could be envisaged.[7] Upon breakage of the TMG ring C–O bond in the Py,TMG complex, the ring oxygen increases its basicity, and the H of the TMG–OH simultaneously becomes more acidic. The travel along the reaction coordinate thereby makes the potential in which the hydrogens move more symmetrical. As the symmetry increases, the bond strength of the two hydrogen bonds also increases. Kreevoy and co-workers have found that strong hydrogen bonds can be described by double-well potentials having such small barriers between the wells that the first vibrational level is above the barrier, i.e., the motion of the hydrogens is not controlled by a barrier.[38] In the A-S_E2 mechanism of acetal hydrolysis, a high-energy intermediate is formed and its formation is facilitated by general acid catalysis. In the transformation of the Py,TMG complex to the hydroxy aldehyde 2-hydroxypyridine complex no such high-energy intermediate is expected to form. It is bypassed by bifunctional catalysis. A comparison of our fractionation factors ϕ_{A1} (0.65) and ϕ_{A2} (0.42)—keeping in mind that their errors could be large—with data presented by Kreevoy[38b] and others[18] does not unequivocally select any of the two types of potentials. However, mechanisms involving consecutive hydrogen transfers in which the transfer of either one—coupled to heavy-atom motion—is rate controlling are considered unlikely on the basis of the magnitudes and similarity of the measured fractionation factors. If one of the fractionation factors in a stepwise mechanism is assumed to be equal to 1 (which corresponds to k_{HH}/k_{HD} or k_{HH}/k_{DH} equal to 1, and to a weak hydrogen bond), then with our data the other factor becomes 0.27. However, in this case it is not the curved but the straight dashed line of Figure 2 that represents the result. If we allow the hydrogen bond involving the hydrogen not in transit to increase in strength, then its fractionation factor is expected to decrease and consequently the other one to increase, i.e., the change is in the direction of our observations.

From our discussion it is apparent that the picture that emerges for the reaction mechanism is not a sharp one. However, all the evidence collectively favors a mechanism in which the two hydrogens are transferred simultaneously with their motion considerably coupled to heavy-atom motion. In the transition state either the transfer of the hydrogens could be governed by a potential with a barrier or their motions could take place without barrier control.

It is appropriate to make some comments on the "primary" isotope effect on the "uncatalyzed" mutarotation, which is about 4.5 (cf. entries 7 and 8 in Table I). This isotope effect is not far from $k_{HH}/k_{DD} = 3.7$ obtained for the title catalysis. At present we can only speculate about the mechanism for this "blank" epimerization since we do not know if traces of water catalyze the reaction or not. However, a possibility is that the epimerization takes place in a TMG dimer and that both ring C–O bonds are broken simultaneously while the two hydrogens are transferred.

Acknowledgment. For financial support, we thank the Swedish Natural Science Research Council and, with respect to the isotope effect calculations, the U.S. National Science Foundation.

Registry No. 1 (α isomer), 6163-35-5; 1 (β isomer), 19146-17-9; **2**, 35510-38-4; **3** (α isomer), 85736-36-3; **3** (β isomer), 85736-37-4; 2-pyridinone, 142-08-5; deuterium, 7782-39-0.

---

[37] (a) Schowen, R. L. *Prog. Phys. Org. Chem.* **1972**, *9*, 275. (b) Schowen, K. B. Ph.D. Thesis, Massachusetts Institute of Technology, 1964.

[38] (a) Kreevoy, M. M.; Liang, T.; Chang, K.-C. *J. Am. Chem. Soc.* **1977**, *99*, 5207–5209. (b) Kreevoy, M. M.; Liang, T. M. *Ibid.* **1980**, *102*, 3315–3322. (c) Kreevoy, M. M.; Ridl, B. A. *J. Phys. Chem.* **1981**, *85*, 914–917.